

# Frequency response analysis of shape memory alloy actuators

Yee H. Teh\* and Roy Featherstone

Dept. Information Engineering, RSISE, Australian National University, Canberra,  
ACT 0200, Australia

## ABSTRACT

This paper presents a frequency response analysis of nickel-titanium Shape Memory Alloy (SMA) wires that are the active elements in an SMA actuator. Frequency response analysis is the measurement of the relative magnitude and phase of an output signal, with respect to an input signal, at spot frequencies covering a frequency range of interest. In this case, the input signal is the electrical heating power applied to the SMA wire, the output is the tensile force on the wire, and the frequency range is 0.1 Hz to 100 Hz. The purpose of such measurements is to obtain a transfer function, relating power input to force output, that can be used to design a feedback control system for a precision SMA force actuator. Measurements are presented for wires having diameters of 75, 100 and 125  $\mu\text{m}$ , in ambient air at room temperature, under various combinations of stress and strain. It is shown that the phase response is independent of stress and strain, while the magnitude response varies by about 7 dB.

**Keywords:** Shape Memory Alloys, actuators, frequency response analysis, force feedback control

## 1. INTRODUCTION

Consider an actuator that produces a force in response to a command signal. The active element in this actuator is a wire made of a Shape Memory Alloy (SMA) that contracts when it is heated, so that heating increases the tension on the wire. The wire is heated electrically, and it cools by convection to its surroundings. If the actuator's output force is to track the command signal accurately, then a force sensor is required, and a feedback control system must be used to adjust the heating power as a function of the difference between the commanded and measured forces. Unfortunately, the design of control systems for SMA actuators has proven to be difficult. Many designs have been proposed in the literature,<sup>1-4</sup> mostly for position control, but they suffer from various deficiencies, such as slow speed and limit cycles (oscillating around the commanded position instead of converging to it).

To design a high-performance feedback control system, it is very helpful to have a dynamic model of the plant (the system being controlled); in this case, a model relating the tension force on the wire to the applied heating power. This paper presents a method for obtaining such a model, using a technique called frequency response analysis.<sup>5</sup> This technique involves applying a small sinusoidal input to the plant, measuring the magnitude and phase of the sinusoidal component of the output, and repeating at various different frequencies covering a desired frequency range. The input signal is kept small so as to measure the small-signal response of the plant. This is important because the large-signal behaviour of SMA is highly nonlinear and hysteretic, but its small-signal behaviour is relatively linear and exhibits relatively little hysteresis.<sup>6,7</sup> A model is then constructed in the form of a transfer function that matches the measured gain and phase data over the frequency range of interest. Such a model describes only the AC behaviour of the wire, not its DC behaviour. However, we have found that this is actually an advantage, as the AC behaviour is more repeatable, and therefore more reliable, than the DC behaviour.

The experiments in this paper investigate the frequency response of a commercial brand of nickel-titanium SMA, called Flexinol, which is specifically made for use in actuators. Wires having diameters of 75  $\mu\text{m}$ , 100  $\mu\text{m}$  and 125  $\mu\text{m}$  were used, and their responses were measured in the frequency range of 0.1 to 100 Hz. At first sight, 100 Hz may seem rather high. However, these wires do exhibit a detectable response even at frequencies above 1 kHz.<sup>8</sup> Furthermore, in terms of controlling SMA actuators, even quite small high-frequency effects are capable of destabilising a closed-loop system. Our earlier experiments on position control of SMA actuators showed limit cycles at frequencies as high as 30 Hz.<sup>9</sup>

---

\*yee.teh@rsise.anu.edu.au; phone 61 2 6125 8821; fax 61 2 6125 8660

Copyright 2007 Society of Photo-Optical Instrumentation Engineers. This paper was published in Proc. Int. Conf. Smart Materials and Nanotechnology in Engineering, Harbin, China, 1-4 July 2007, and is made available as an electronic reprint with permission of SPIE. One print or electronic copy may be made for personal use only. Systematic or multiple reproduction, distribution to multiple locations via electronic or other means, duplication of any material in this paper for a fee or for commercial purposes, or modification of the content of the paper are prohibited.

The final section in this paper describes a transfer function model that was obtained from the experimental data for the 100  $\mu\text{m}$  diameter wire. This modelling approach can assist us in designing fast and highly accurate force control systems, as have been shown for a single-wire SMA actuator,<sup>10</sup> as well as an actuator based on an antagonistic pair of SMA wires.<sup>11</sup> Potential applications may include camera anti-shake mechanisms, active vibration control, SMA-actuated grippers and other actuator applications.<sup>12–15</sup>

The contributions of this paper are as follows: it describes a new way to characterise the dynamic behaviour of SMA wires that is particularly useful for designing control systems; and it validates this method by experiment. The results reveal the following previously-unknown properties of SMA wires: the phase response is independent of stress and strain; the effect of stress and strain on the magnitude response is independent of frequency; and the magnitude response exhibits a single pole that decreases in frequency as the diameter increases.

## 2. EXPERIMENTAL SETUP

### 2.1 Experimental Apparatus

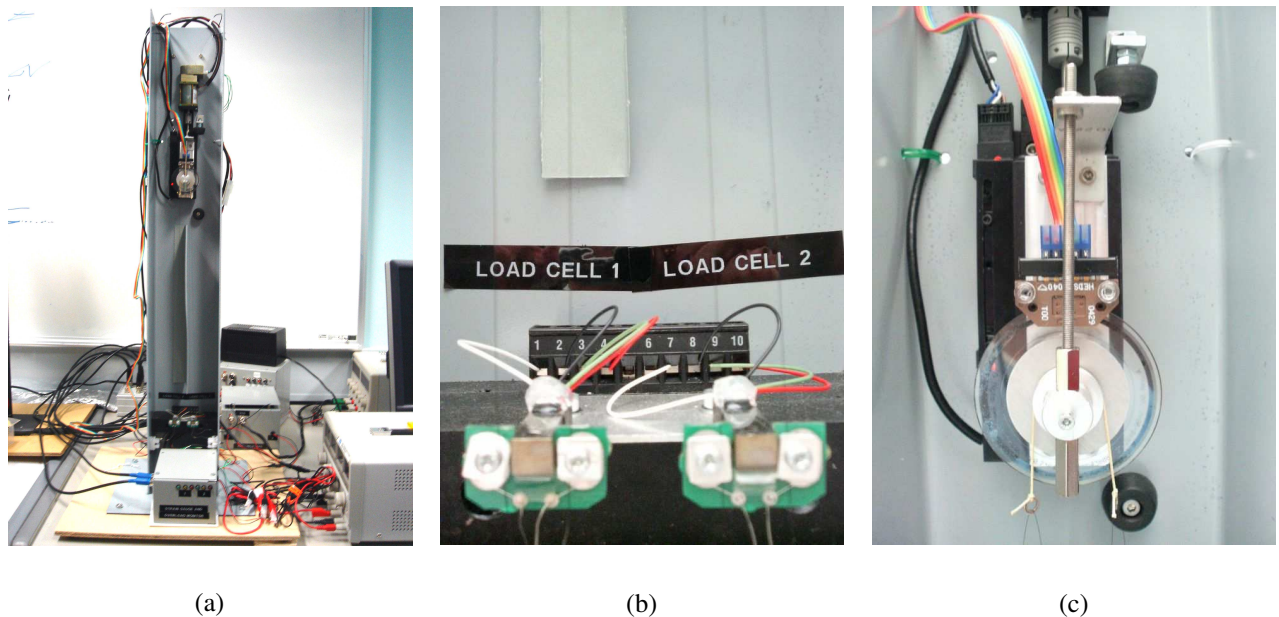


Figure 1. The experimental test bed (a), and detailed views of the load cell housings (b) and the linear slide (c).

The small-signal frequency response analysis has been conducted using the test bed shown in Figure 1. The test bed can accommodate pairs of SMA wires arranged antagonistically about a rotating pulley and shaft housing. However, only single wires were used in these experiments. Three different diameters were investigated: 75  $\mu\text{m}$ , 100  $\mu\text{m}$  and 125  $\mu\text{m}$ . The wires are made of Flexinol\* with an austenite finish temperature of 90°C. These are commercially produced NiTi alloy wires capable of contracting millions of times, with a normal working strain of 4%. The wires in our test bed are 80 cm long.

The major components of the test rig are: (1) two S215 load cells<sup>†</sup> capable of accurate force measurements in the  $\pm 9\text{ N}$  range with a resolution of 0.3 mN and a bandwidth of 140 Hz, (2) a servo-controlled precision linear slide capable of applying precise strain profiles to the SMA wires, (3) precision DC current amplifiers for heating the SMA wires, and (4) a DS1104 real-time control board from dSPACE upon which experiments and control systems can be implemented using *MATLAB/Simulink*<sup>TM</sup>. In the experiments reported here, the DS1104 ran at a sampling rate of 10 kHz.

The two load cells, one for each SMA wire, are housed at the bottom of the test rig as shown in Figure 1(b). Visible in this figure, each SMA wire is doubled-up, so that both ends are electrically connected to a tiny printed circuit board attached at the end of each load cell. Note that only one wire is used at a time for this analysis.

The linear slide is positioned at the top of the test rig as shown in Figure 1(c). The slide also houses the rotating pulley and shaft with a pulley-locking mechanism and an optical shaft encoder. The pulley is intended for use with

\*Flexinol is a trademark of Dynalloy, Inc. (<http://www.dynalloy.com>)

<sup>†</sup>S215 load cells obtained from Strain Measurement Devices. (<http://www.smdsensors.com>)

antagonistic pairs of SMA wires. For the experiments described in this paper, the pulley is locked mechanically as shown in Figure 1(c).

## 2.2 Experimental Procedures

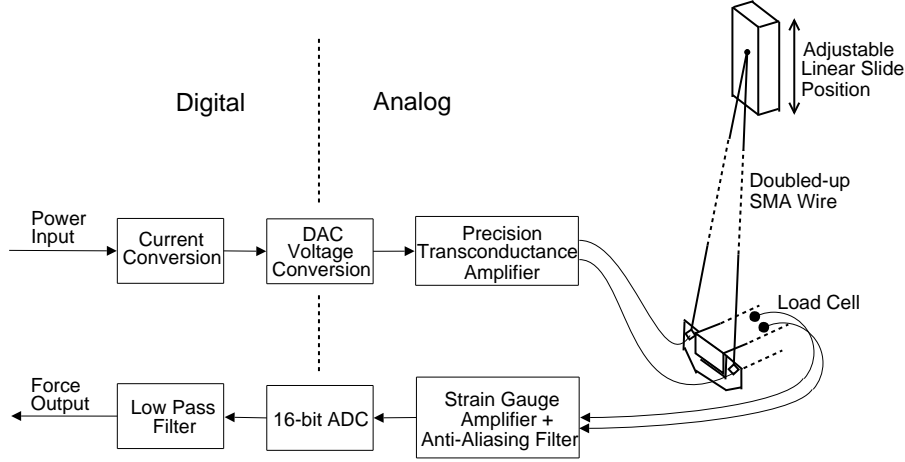


Figure 2. Experimental system.

Figure 2 presents a simplified block diagram of the experimental system. Firstly, a signal of the form  $a + b \sin(\omega t)$  is generated, where  $a \geq b$ . This signal represents the heating power to be applied to the wire.  $a$  is the mean power, and  $b$  the magnitude of the sinusoidal component. This signal is converted to a current signal using a nominal value for the wire's electrical resistance, and is then converted to an analog voltage and sent to the precision current amplifier, which drives the SMA wire. The measured force is obtained from the load cell using a 16-bit analog-to-digital converter and is low-pass filtered to remove unwanted high-frequency noise. Once steady-state is achieved, the force signal is recorded for a sufficient length of time to allow an accurate measurement of the magnitude and phase of the sine-wave component at the driving frequency,  $\omega$ . The above procedure is repeated for suitable spot frequencies over the 0.1 – 100 Hz range.

It should be noted that the mean (DC) value of the input power signal is kept constant over the frequency range so that the mean force output is fairly constant, although the magnitude of the AC input signal is varied. At the lowest frequency, the magnitude of the sinusoid is kept small, so that only small temperature variations result; but the magnitude is increased at higher frequencies so that there is still a detectable force signal. Strictly speaking, it is the temperature fluctuation that is the small signal, not the heating power. However, input power rather than temperature is used as the experimental parameter because of the difficulty of measuring rapidly-varying temperature for a thin wire. The SMA wire is also shielded within the test bed to reduce the effects of air ventilation on wire temperature.

The next step is to extract the sine-wave component in the recorded data at the driving frequency  $\omega$ , and measure its magnitude and phase. This is accomplished using a recursive parameter identification method based on a least-squares algorithm.<sup>16</sup> This algorithm is robust, and the calculated magnitude and phase are accurate, in spite of noise and harmonic distortion in the recorded data, because the algorithm calculates an average over many cycles of the driving frequency. The estimation of the force amplitude and phase is conducted using the *Adaptive Control Toolbox* in *MATLAB/Simulink*<sup>TM</sup>. At the end of this process, we have a set of magnitude and phase data for one wire diameter, at one particular strain and average stress condition.

The procedure is then repeated using different mean values of the input power signal and varying linear slide positions to produce a variety of stresses and strains in the wire, spanning the full range of allowable stresses and strains. The whole experiment is then repeated using wires of different diameters.

## 3. RESULTS AND DISCUSSIONS

### 3.1 Frequency Response Results

Figure 3 shows the experimental Bode plots of the system using different wires diameters of 75  $\mu\text{m}$ , 100  $\mu\text{m}$  and 125  $\mu\text{m}$  under varying stress and strain conditions. Each curve represents one stress-strain combination. The magnitude in decibels (dB) is given by:

$$\text{Magnitude} = 20 \log \frac{\text{Force Amplitude}}{\text{AC Power}}, \quad (1)$$

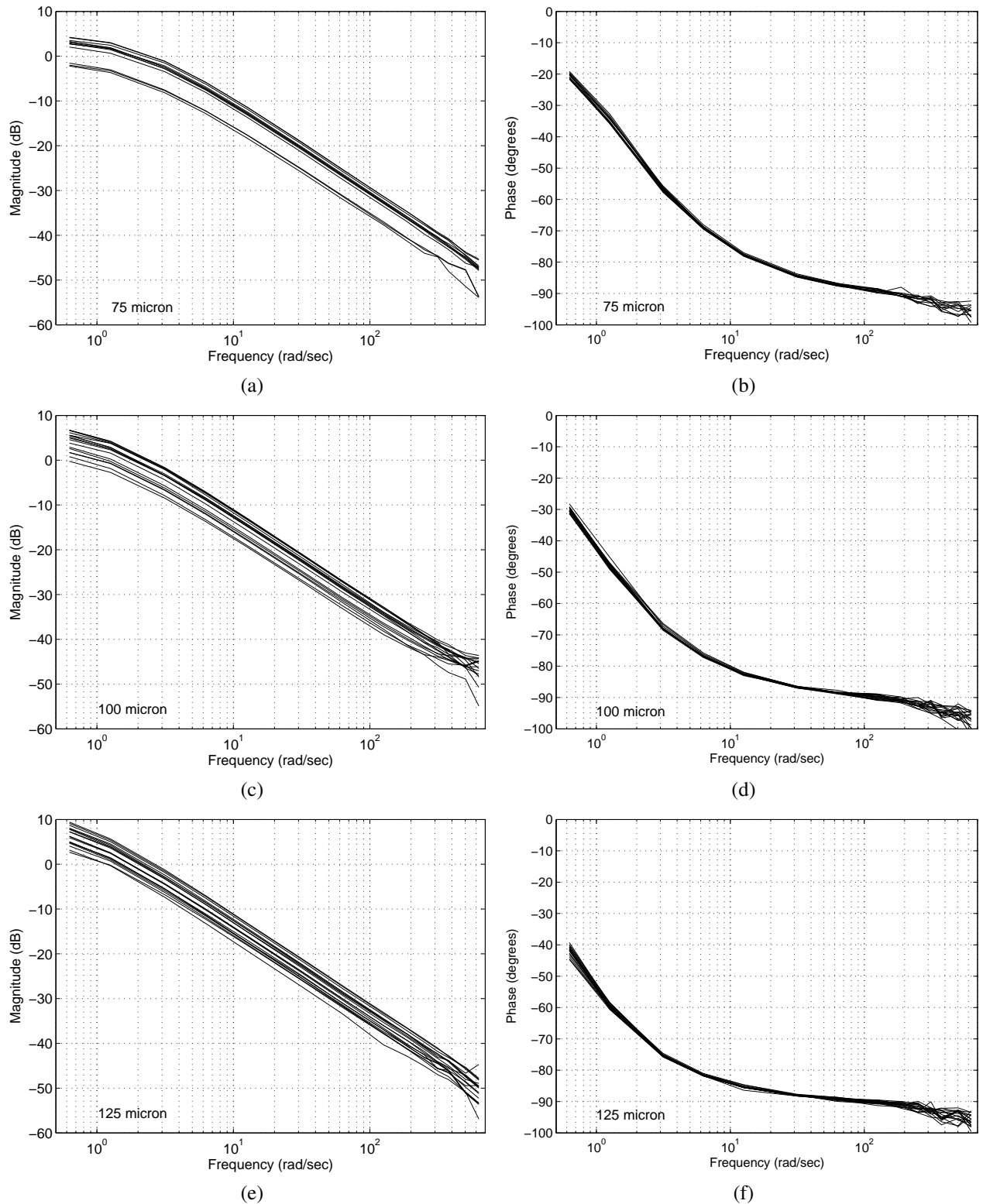


Figure 3. Bode magnitude and phase plots for Flexinol wires having diameters of 75  $\mu\text{m}$ , 100  $\mu\text{m}$ , and 125  $\mu\text{m}$ .

where the force amplitude is the least-squares estimate calculated using the best-fit sinusoid and the AC power is the parameter  $b$  mentioned in Section 2.2. The phase in degrees ( $^\circ$ ) is the phase shift between the best-fit sinusoid and the input power signal. As a final processing step, the magnitude and phase data are adjusted to compensate for the known transfer functions of the low-pass filter and the anti-aliasing filter, as well as the measured mechanical resonance (at

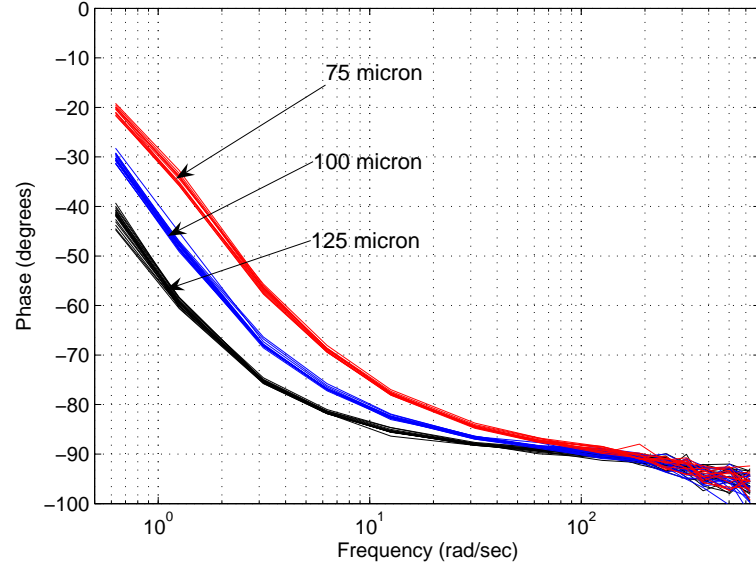


Figure 4. Superimposed phase plots for Flexinol wires of different diameters.

280 Hz) in the load cells.

The most striking feature of Figure 3 is that the phase response is independent of stress and strain for each wire diameter. If we plot the three sets of phase curves in a single graph, as in Figure 4, then it can be seen that they are shifted horizontally relative to each other, and that they converge to a phase lag of  $90^\circ$  at high frequencies. This is the behaviour that one would expect of a linear, first-order, low-pass filter with a cut-off frequency that decreases with increasing wire diameter.

The magnitude response graphs show a different picture. For any given diameter, the curves all have almost the same shape, but are vertically shifted relative to each other within a window of approximately 7 dB. This shows that any change in stress or strain has approximately the same effect at all frequencies. The magnitude response curves for the  $75\ \mu\text{m}$ -diameter wire are almost horizontal at the lowest frequencies, but switch to a slope of approximately  $-20\ \text{dB}$  per decade at a frequency of about  $2\ \text{rad s}^{-1}$ . This frequency, at which the change of slope occurs, is known as a pole.<sup>5</sup> The magnitude responses for the other two diameters are the same, except that the pole appears at progressively lower frequencies as the diameter is increased. This pole probably marks the boundary between frequencies at which the wire is substantially at thermal equilibrium and frequencies at which it is not.

The experiment in this paper investigated only a narrow range of diameters. It is therefore difficult to speculate on what might happen at diameters that are very much larger or smaller than those investigated here. Nevertheless, it is reasonable to suppose that the pole will continue to rise as the diameter is reduced below  $75\ \mu\text{m}$ , and continue to fall as the diameter is increased above  $125\ \mu\text{m}$ .

### 3.2 Modelling

Let  $P(s)$  and  $F(s)$  denote the Laplace transforms of the heating power and measured force signals, respectively. The dynamic behaviour of an SMA wire can be modelled by a transfer function,  $G(s)$ , which satisfies

$$F(s) = G(s)P(s). \quad (2)$$

To model the  $100\ \mu\text{m}$  wire data in Figure 3, we chose a first-order linear transfer function. The analytical expression for this transfer function is

$$G(s) = \frac{K}{Ts + 1}, \quad (3)$$

and a suitable value that fits the experimental data is

$$G(s) = \frac{1.7}{0.7579s + 1}. \quad (4)$$

Grant and Hayward had also observed and modelled similar first-order behaviour in their SMA actuator response.<sup>7</sup> The Bode magnitude and phase plots for our model are shown as the dashed black curves in Figure 5. The model can be

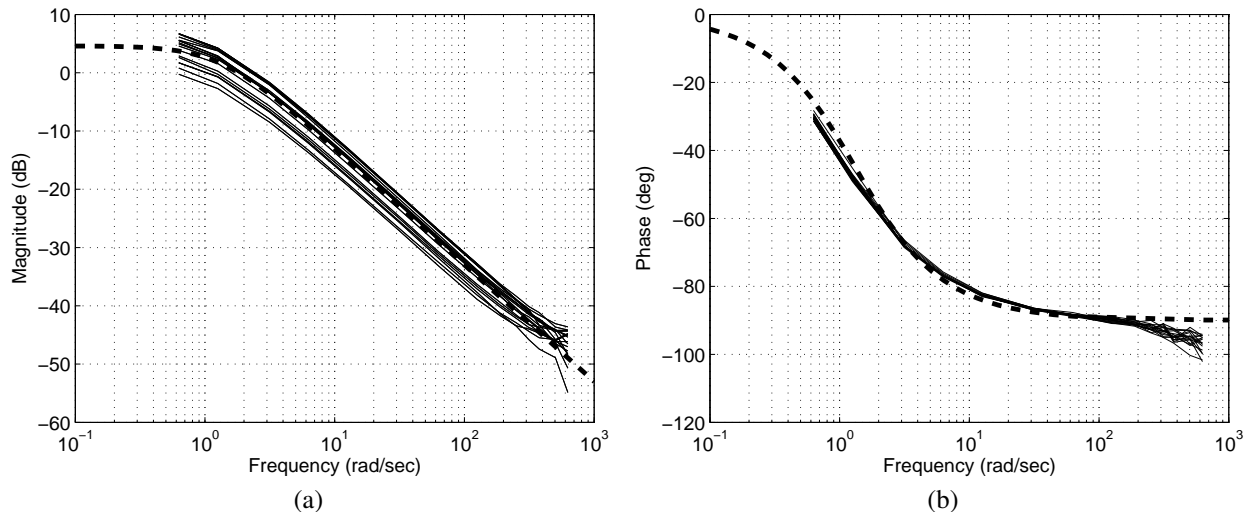


Figure 5. Bode magnitude and phase plots of the 100  $\mu\text{m}$ -diameter Flexinol wire frequency response data and the derived transfer function model,  $G(s)$ . Solid black lines = experimental data. Dashed black line = model.

observed to reasonably match the experimental Bode plots over the entire frequency range. Similar models can be determined for other wire diameters. Such models extracted from the frequency response analysis can be used to design stable, accurate feedback control systems for SMA actuators.<sup>10,11</sup>

#### 4. SUMMARY

This paper describes a new method of characterising the dynamic behaviour of SMA wires based on small-signal frequency response analysis. Over a frequency range of 0.1 Hz to 100 Hz, detectable force responses from SMA wires are recorded and then processed to produce sets of Bode diagrams for different diameters of 75  $\mu\text{m}$ , 100  $\mu\text{m}$  and 125  $\mu\text{m}$ . The experimental results show several invariant properties of the magnitude and phase responses, which allows a dynamic force model of the SMA to be determined. This model takes the form of a transfer function, relating the heating power to the output force, and it is particularly useful for the design and simulation of force feedback control systems for SMA actuators.

Future work involves building a position model of the SMA actuator based on the force model. This position model not only takes into account the input heating power, but also strain variations due to contraction and extension. This can be accomplished using frequency response analysis to investigate the effects of small continuous strain changes to the SMA dynamic behaviour. Faster and more accurate position feedback controllers can be designed and tested with the aid of the model.

#### REFERENCES

1. D. Grant and V. Hayward, "Variable structure control of shape memory alloy actuators," *IEEE Systems and Control Magazine*, 17(3), 80-88 (1997).
2. J.L. Pons, D. Reynaerts, J. Peirs, R. Ceres and H. Van Brussel, "Comparison of different control approaches to drive SMA actuators," *Proc. 8<sup>th</sup> Int. Conf. Advanced Robotics*, Monterey, USA, 819-824 (1997).
3. N. Troisfontaine, P. Bidaud and P. Dario, "Control experiments on two SMA based micro-actuators," in *Experimental Robotics V*, A. Casals and A.T. de Almeida (eds.), Springer, 490-499 (1998).
4. H. Ashrafiun, M. Eshraghi and M.H. Elahinia, "Position control of a 3-link shape memory alloy actuated robot," *J. Intelligent Mat. Sys. and Struct.*, 17, 381-392 (2006).
5. G.F. Franklin, J.D. Powell and A. Emami-Naeini, *Feedback Control of Dynamic systems*, 3<sup>rd</sup> ed., Addison-Wesley Publishing Group, 1994.
6. K. Kuribayashi, "A new actuator of a joint mechanism using Ti-Ni alloy wire," *Int. J. Robotics Research*, 4(4), 47-58 (1986).
7. K. Kuribayashi, "Micro SMA actuator and motion control," *Proc. IEEE Int. Symp. Micromechatronics and Human Science*, Nagoya, Japan, 35-42 (2000).

8. Y.H. Teh and R. Featherstone, "Experiments on the audio frequency response of shape memory alloy actuators," *Proc. 7<sup>th</sup> Australasian Conf. Robotics and Automation*, Sydney, Australia, 2005.
9. Y.H. Teh and R. Featherstone, "Experiments on the performance of a 2-DOF pantograph robot actuated by shape memory alloy wires," *Proc. 6<sup>th</sup> Australasian Conf. Robotics and Automation*, Canberra, Australia, 2004.
10. Y.H. Teh and R. Featherstone, "Accurate force control and motion disturbance rejection for shape memory alloy actuators," *Proc. IEEE Int. Conf. Robotics and Automation*, Rome, Italy, 4454-4459 (2007).
11. Y.H. Teh and R. Featherstone, "An architecture for fast and accurate control of Shape Memory Alloy actuators," *Int. J. Robotics Research*, (Submitted May 2007).
12. O. Masamichi, *Drive Apparatus, Drive System, and Drive Method*, Konica Minolta Inc., US Patent Number 2006150627, 13 Jul 2006.
13. C. Liang and C.A. Rogers, "Design of shape memory alloy springs with applications in vibration control," *J. Vibration and Acoustics*, 115, 129-135 (1993).
14. M. Kohl, *Shape Memory Microactuators*, Springer, Berlin, 2004.
15. J. Van Humbeeck, "Non-medical applications of shape memory alloys," *Mat. Sci. and Eng. A*, 273-275, 134-138 (1999).
16. P. Ioannou and B. Fidan, *Adaptive Control Tutorial*, SIAM: Society for Industrial and Applied Mathematics, Philadelphia, USA, 2006.